Computers in Biology and Medicine 87 (2017) 271–284

Contents lists available at ScienceDirect

Computers in Biology and Medicine

journal homepage: www.elsevier.com/locate/compbiomed

Classification of ECG heartbeats using nonlinear decomposition methods and support vector machine

Kandala N.V.P.S. Rajesh *, Ravindra Dhuli

School of Electronics Engineering, VIT University, Vellore 632014, India

ARTICLE INFO

Keywords:
ECG signal
Arrhythmia
Empirical mode decomposition
Ensemble empirical mode decomposition
Classification
SMO-SVM

ABSTRACT

Classifying electrocardiogram (ECG) heartbeats for arrhythmic risk prediction is a challenging task due to minute variations in the amplitude, duration and morphology of the ECG signal. In this paper, we propose two feature extraction approaches to classify five types of heartbeats: normal, premature ventricular contraction, atrial premature contraction, left bundle branch block and right bundle branch block. In the first approach, ECG beats are decomposed into intrinsic mode functions (IMFs) using ensemble empirical mode decomposition (EEMD). Later four parameters, namely the sample entropy, coefficient of variation, singular values, and band power of IMFs are extracted as features. In the second approach, the same features are computed from IMFs extracted using an empirical mode decomposition (EMD) algorithm. The features obtained from the two approaches are independently fed to the sequential minimal optimization-support vector machine (SMO-SVM) for classification. We used two arrhythmia databases for our evaluation: MIT-BIH and INCART. We compare the proposed approaches with existing methods using the performance measures given by the average values of (i) specificity, (ii) sensitivity, and (iii) accuracy. The first approach demonstrates significant performance with 98.01% sensitivity, 99.49% specificity, and 99.20% accuracy for the MIT-BIH database and 95.15% sensitivity, 98.37% specificity, and 97.57% accuracy for the INCART database.

1. Introduction

The functioning of the human body is under the profound influence of the heart, which plays a significant role in the cardiovascular system. Any functional limitations in the heart can lead to cardiovascular diseases (CVDs). CVDs are increasing the mortality rate worldwide, especially in the low and middle-income countries [43]. Sudden cardiac arrest due to cardiac arrhythmia is one of the major concerns in these countries. Cardiac arrhythmias occur due to improper electrical conduction or impulse formation in the heart, which can affect heart morphology or disrupt the rate of a regular heartbeat. An arrhythmia can cause abnormal heartbeats such as ectopic and bundle branch block beats. Ectopic beats are formed because of improper electrical impulse formation. Ectopic beats are further classified as premature ventricular and atrial contractions. These beats will disturb the heart's regular rhythm and can induce serious arrhythmias such as ventricular or atrial fibrillation. Bundle branch blocks impede the normal pathway of electrical impulses through the conduction system to the ventricles. This causes asynchronous ventricular contractions and heart function deterioration, which may lead to life-threatening situations [52]. These situations are prompting researchers to investigate both detection and classification methods for cardiac arrhythmias. A sequence of heartbeats can be mapped to an arrhythmia; hence, an important step in detection and classification of arrhythmias is heartbeats characterization [61].

An electrocardiogram (ECG) is a popular diagnostic tool for examining the heart's electrical activity. An ECG signal represents the heart muscle's depolarization and repolarization actions as heartbeats. Manual observation of subtle changes between and within the heartbeats in an ECG is a tedious job. Therefore, by recognizing various kinds of heartbeats, computer-aided diagnosis (CAD) plays an important role in detection and classification of cardiac arrhythmias. This will help cardiologists to monitor physiological conditions of heart activity at regular intervals. This work investigated a method for classification of heartbeats that could help in detecting various types of arrhythmias. The importance of CAD in cardiac arrhythmia detection and classification was demonstrated in previous studies [29,40,41]. An appropriate choice of features and classifiers would improve the classification method. Heartbeat classification methods can be broadly categorized into four groups based on the selection of features [39], viz., time-domain, frequency-domain, time-frequency and nonlinear methods.

* Corresponding author.
E-mail addresses: kandala.rajesh2014@gmail.com (K.N.V.P.S. Rajesh), ravindradhuli@vit.ac.in (R. Dhuli).

http://dx.doi.org/10.1016/j.compbiomed.2017.06.006
Received 14 February 2017; Received in revised form 3 June 2017; Accepted 3 June 2017

In the time-domain, linear prediction [36], ECG morphology, R-R intervals [13] and linear discriminant analysis (LDA) [63] are used. In frequency-domain, feature extraction methods based on Fourier transform [44], subband decomposition [2] and non-parametric power spectral density (PSD) [30] were explored for heartbeat discrimination. Time-frequency approaches are popular because of their multi-resolution analysis capabilities. Afonso and Tompkins [1] used short time Fourier transform (STFT) and Wigner-Ville distribution (WVD) to discriminate shockable rhythms from non-shockable cardiac rhythms. Wavelets are also widely used in this context [3,27,31,42]; however, the reasons behind rhythmic and wave shape changes in ECG are complicated. Deviation from the rhythmic activity in the ECG signal is called arrhythmia. Arrhythmias are considered being caused by pathological conditions, such as disturbances in the autonomic nervous system, dysfunctions of natural pacemakers, or failures in the electrical conduction pathway in the myocardium. The ECG signal results from combining signals from mutually related and inherently nonlinear biological systems. Hence, to analyze this, we need a decomposition technique that is nonlinear and adaptive.

Researchers attempted to decompose ECG into various modes using some basis functions [26,40]. Nonlinear features, like higher-order cumulants [42,64] and approximate entropy [34] are extracted from these modes. However, these basis functions are not dynamic and thus unable to meet morphological changes. There is a need for an adaptive mechanism to decompose the ECG signal. A popular analysis tool known as ensemble empirical mode decomposition (EEMD) [59] is used in this work. EEMD decomposes non-stationary signals originating from nonlinear systems into intrinsic mode functions (IMFs), depending on the signal characteristics, without depending on any prior basis. These modes are regular and spread across the whole time span with similar scales [12]; therefore, EEMD will give the subtle information of a signal, in terms of modes. EEMD has shown its potentiality in a variety of applications, including fault diagnosis in mechanical applications [15,32,33], ECG filtering [10] and seismic signal analysis [58]. So far, EEMD is not exploited in ECG signal classification. In this paper, we attempt to classify five types of morphological heartbeats (normal, PVC, APC, LBBB and RBBB) based on their EEMD features. Classifier selection is crucial in the detection and classification problem; different classifiers were used in the literature, including self-organizing maps (SOM) [7], k-nearest neighbor [26], ANN's [21,47] and cluster analysis [62]. In this paper, we used a sequential minimal optimization-support vector machine (SMO-SVM) for classification. Martis et al. [39] reported that in certain cases, nonlinear methods perform well even under noisy conditions [28,54]; therefore, we tested the performance of our method in the presence of noise.

This paper is structured as follows. Section 2 provides information regarding the dataset used in this work also presents the proposed method including pre-processing, feature extraction and classification. Description about the experiment and discussion on the obtained results are presented in Section 3. Conclusion is presented in Section 4.

2. Methodology

For analyzing the proposed method, we chose the database from the Massachusetts Institute of Technology-Beth Israel Hospital (MIT-BIH) arrhythmia database [45]. In this database, several types of heartbeats obtained from male and female patients are stored in 48 records. Each record duration is 30:06 min sampled at 360 Hz. From the collected data, five types of heartbeats: normal, PVC, APC, LBBB and RBBB are used for classification. Details of these data are provided in Table 1. The proposed methodology is elucidated below.

Table 1
Number of beats used in this work.

Type of ECG beat	Number of beats	Record name
Normal (N)	2000	100,101,108,112
Premature Ventricular Contraction (PVC)	2000	106,107,200,201
Atrial Premature Contraction (APC)	2000	100,101,103,108,112,114,116, 118,121,124,200,201,202,205, 207,209,213,215,219,220,222, 223,228,231,232,233
Left Bundle Branch Block (LBBB)	2000	109,111,207,214
Right Bundle Branch Block (RBBB)	2000	118,207,212

In general, automatic heartbeat classification system comprises three building blocks: pre-processing, feature extraction and classification as shown in Fig. 1. We will discuss the details of the approaches and also the theoretical background of the employed techniques.

2.1. Pre-processing

Pre-processing consists of denoising and segmentation parts.

2.1.1. Denoising

For an accurate diagnosis, clinicians always prefer noise free ECG signals. However, in real time scenario, ECG recordings have inherent artifacts. Prominent among them are high frequency noise due to power line interference and low frequency noise such as baseline wander due to motion or respiration of the patient. Hence, it is advisable to first denoise the ECG records. For denoising the filtering technique proposed by Ref. [5] is used with slight modification.

This method consists four steps:

1. Eliminate the mean bias from the noisy ECG signal.
2. Moving average filter with order five (cut-off frequency = 24 Hz) is used for eliminating the high frequency components due to power line interference and muscle noise.
3. High-pass filter with cut-off frequency 1 Hz is used for baseline wander suppression.
4. Additional low-pass filter with cut-off frequency 45 Hz is used to further suppress any left out high frequency artifacts, since most of the ECG signal energy lies between 0.5 and 45 Hz [60].

Segmentation follows the denoising mechanism.

2.1.2. Segmentation

ECG signal obtained after denoising has to be segregated into individual heartbeats. Two major approaches available for this purpose are (1) detecting the QRS complex, (2) using the annotation files provided by the experts.

QRS complexes can be detected using various algorithms such as [24,38,46,49].

In our analysis, we make use of MIT database annotation files [11,14,29]. To obtain a heartbeat, a window of length 300 is applied on ECG signal. These beats from each class are presented in Fig. 2 with the corresponding time axis. By observing Fig. 2, large morphological variations among and within the normal and abnormal heartbeats can be observed. A major problem for the automated ECG beat classification is uncertain ECG morphology. It can be different even within a patient record. But, there is a possibility that it is similar to a different type of ECG beat [48]. This situation can be handled by choosing appropriate features.

2.2. Feature extraction

With the help of feature extraction, we can represent a large data in a few samples, often called, features. Choosing appropriate features will improve the performance accuracy. As shown in Fig. 1, we implement feature extraction in two stages.

In stage one, ECG beats are decomposed into IMFs using EEMD and EMD.

In stage two, sample entropy, the coefficient of variation, singular values and band power values are calculated from IMFs for subsequent analysis.

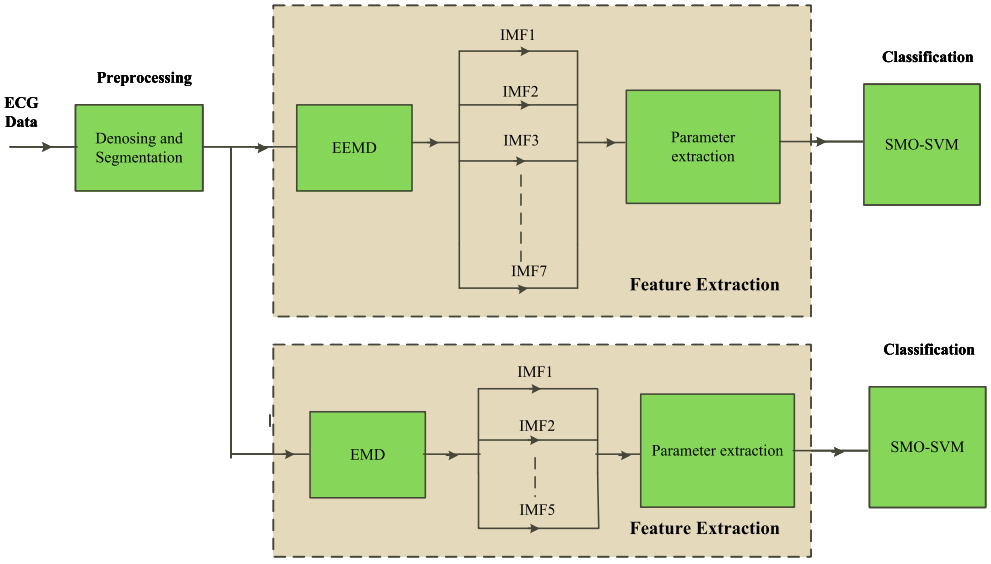

Fig. 1. Block diagram of the proposed methodology.

2.2.1. Empirical mode decomposition (EMD)

EMD is a popular decomposition method well suited for non-stationary data stemming out of nonlinear systems [22]. Unlike wavelet transform, EMD decomposes data into IMFs which are amplitude and frequency modulated (AM-FM) functions. EMD exploits the local information contained in the data itself [25]. IMF which is treated as a basis function, holds the local oscillation information of the signal.

IMF must satisfy two conditions:

i. The number of extrema and the number of zero-crossings in data segment must be similar or at most differ by one.
ii. At any time instant, the local mean values of the upper and lower envelopes defined by local extrema must be zero [12].

EMD process generates IMFs using the sifting process described in Algorithm 1 [22]. EMD process starts with identifying the extrema (local minima and local maxima) for a given signal $x(t)$.

Algorithm 1 EMD

Step 1: Initialize: $r_0(t) = x(t)$, and $l = 1$.
Step 2: Initialize: $h_{l,k}(t)=r_{(l-1)}(t)$, $k = 0$
Step 3: Find extrema of $h_{l,k}(t)$
Step 4: Compute upper and lower envelopes $e_{U,l,k}(t)$ and $e_{L,l,k}(t)$ by connecting all local extrema using cubic spline interpolation.
Step 5: Compute mean of envelopes,

$$m_{l,k}(t) = \frac{1}{2}\left[e_{U,l,k}(t) + e_{L,l,k}(t)\right]. \tag{1}$$

Step 6: Update proto mode component,

$$h_{l,(k+1)}(t) = h_{l,k}(t) - m_{l,k}(t). \tag{2}$$

Step 7: Calculate

$$SD = \sum_{t=0}^{T} \frac{\left[h_{l,k}(t) - h_{l,(k+1)}(t)\right]^2}{h_{l,k+1}^2(t)}. \tag{3}$$

If $0.2 \leq SD \leq 0.3$, $h_{l,(k+1)}$ is an IMF, save $c_l(t) = h_{l,(k+1)}(t)$ else go to step 3 with $k = k + 1$.
Step 8: $r_l(t) = r_{l-1}(t) - c_l(t)$
Step 9: If $r_l(t)$ has more than one extrema then go to step 2, with $l = l + 1$, else $r_{l+1}(t)$= residue of the signal.

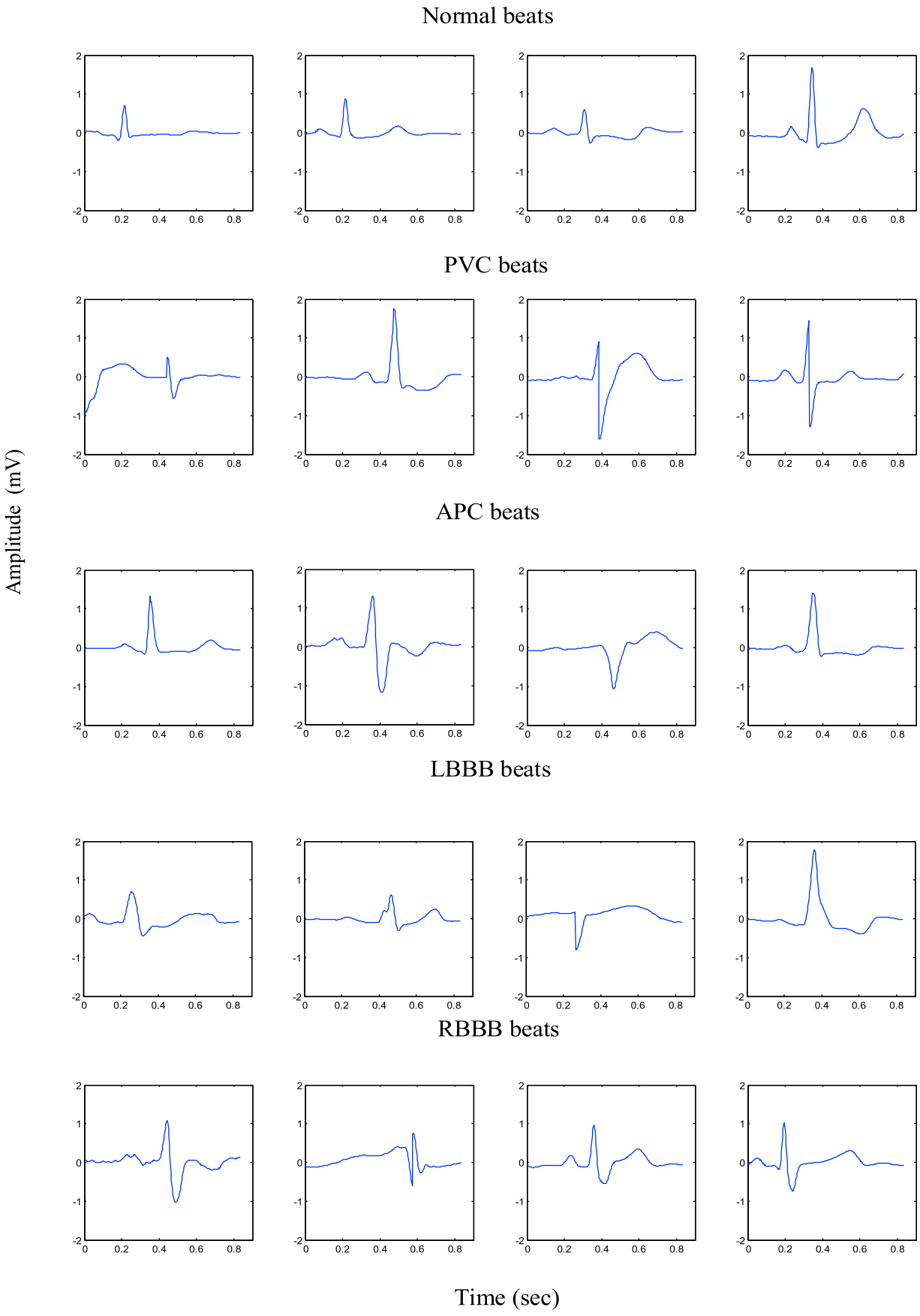

Fig. 2. Segmented beats from Normal, PVC, APC, LBBB, RBBB with 0.83 s (300 data points).

This algorithm is illustrated in Figs. 3 and 4. A normal ECG beat obtained from MIT database is represented in Fig. 3(a). Fig. 3(b) represents the normal ECG beat, upper and lower envelopes and the mean of the envelopes. Proto component $h_{11}(t)$ from Eq. (2), extracted by subtracting the mean of the envelopes from normal ECG beat is shown in Fig. 3(c).

Ideally, $h_{11}(t)$ should be an IMF. However, $h_{11}(t)$ is not satisfying the requirements of an IMF. There are still multiple extrema in between zero crossings. Hence, the iteration process has to be repeated. Fig. 4 depicts the second iteration process. Proto component $h_{11}(t)$, envelopes (upper and lower) of the proto component and mean of the envelopes are shown in Fig. 4(a) and $h_{12}(t)$ is shown in Fig. 4(b). The result is still not an IMF. Therefore, this iteration process is repeated k times. This phenomenon is known as sifting operation. Fig. 4(c) represents the first IMF component achieved after 72 siftings based on the stopping criteria. This operation is continued until the final IMF component becomes residue of the signal.

Using EMD algorithm we can express $x(t)$ as

$$x(t) = \sum_{l=1}^{K} c_l(t) + r_K(t), \tag{4}$$

where c_l is the l^{th} IMF, $r_K(t)$ is the final residue. To illustrate the EMD, we present the decomposition of normal beat and four abnormal beats in Fig. 5.

2.2.2. Ensemble empirical mode decomposition (EEMD)

The main advantage of EMD is its capability to segregate stationary and non-stationary components from any complex data [17]. However, it has a serious limitation of mode mixing i.e., different spectral information combining in one mode. To resolve this issue, a new noise-assisted data analysis method called EEMD came into the picture. EEMD gives the true IMF components. Computing true IMFs using EEMD is described in Algorithm 2 [59]:

Algorithm 2 EEMD

Step 1: Add different copies of zero mean white noise to the original signal .

$$x^i(t) = x(t) + w^i(t), \tag{5}$$

where $w^i(t)(i = 0, 1, ..., M)$ are different copies of white noise with zero mean and standard deviation ε.

Step 2: Perform EMD on each ensemble signal $x^i(t)$ to obtain the modes $c_k^i(t)$, where $k = 1, 2, ..., K$.

Step 3: Compute the k^{th} mode of $x^i(t)$ as the average

$$\overline{c_k(t)} = \frac{1}{M}\sum_{i=1}^{M} c_k^i(t). \tag{6}$$

In this work, we used $\varepsilon = 0.2$. We use both EEMD and EMD to decompose the segmented ECG beats into IMFs for subsequent feature extraction. We consider first seven IMFs in the EEMD analysis and first five IMFs from the EMD method. The number of IMFs is chosen based on the tolerable level of reconstruction error. Fig. 6 depicts the decomposition of normal and four types of abnormal beats using EEMD. We have used EMD toolbox [16] for implementing this algorithm.

2.2.3. ECG parameters

Various parameters are extracted from ECG to generate feature vectors for the classification mechanism. These parameters are calculated from IMF1-IMF7 for EEMD and IMF1-IMF5 for EMD. A brief discussion of these parameters is presented here below.

Sample entropy (SampEn): Sample entropy is a measure of regularity of a time series used to quantify the complexity of heartbeat dynamics [53]. High value of SampEn represents more irregularity in time series. SampEn is often used in the analysis of physiological time series [4,35].

Coefficient of variation (CV): The coefficient of variation is a statistical parameter defined as the ratio of the square of the standard deviation to the square of the selected IMF mean.

$$CV = (\sigma/\mu)^2, \tag{7}$$

where

$$\mu = \frac{1}{L}\sum_{l=1}^{L} c_k(l)\ , \sigma = \left[\frac{1}{L}\sum_{l=1}^{L}(c_k(l) - \mu)^2\right]^{1/2} \tag{8}$$

$L = 300$, $c_k(l)$ is the l^{th} element of IMF vector $\mathbf{c}_k$.

CV is also known as the coefficient of dispersion (or) relative standard deviation since, it compares the degree of dispersion from normal ECG beats to abnormal ECG beats [8,37].

Singular values: The singular value decomposition [19] of a matrix A of size $m \times n$ can be represented as

$$A = U\Sigma V^T. \tag{9}$$

Here U and V are orthogonal matrices and Σ is a diagonal matrix consisting singular values.

$$\Sigma = Diag(\sigma_1, \sigma_2, ..., \sigma_p), \tag{10}$$

where, $\boldsymbol{\sigma} = [\sigma_1, \sigma_2, ..., \sigma_p]^T$ are singular values. We employed singular values as features and calculated them from the selected IMF vectors. These values describe the energy distribution of different modes. They are capable of distinguishing different pathologies in various studies [9,54]. In this work we choose $A = \mathbf{c}_k$.

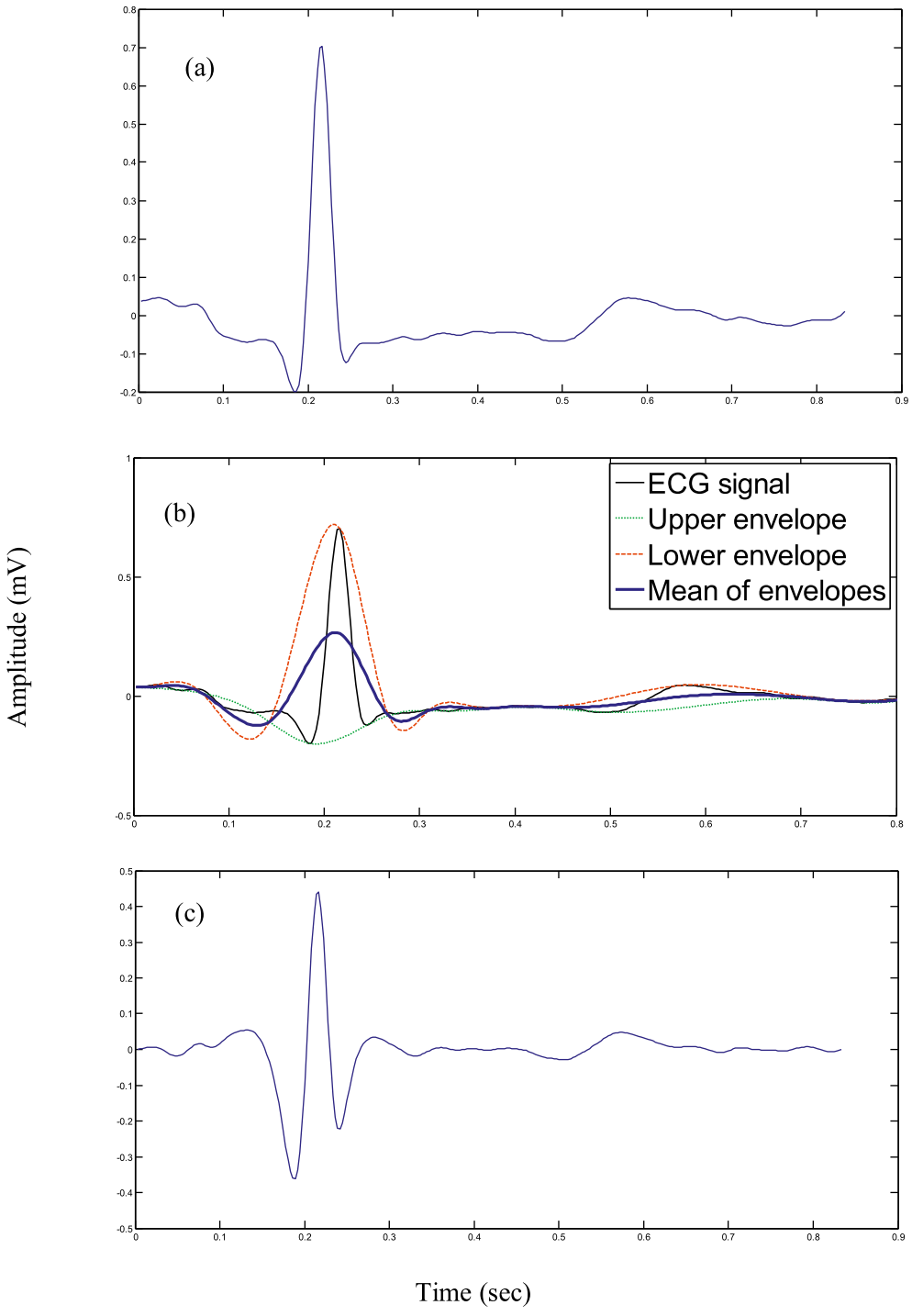

Fig. 3. Illustration of sifting process: (a) normal ECG beat (b) upper and lower envelopes and the mean signal of ECG beat (c) h_{11} component.

Band power (BP): Band power is the average power of each IMF. Let $\mathbf{c}_k$ be one IMF of length L. Then

$$BP = \frac{c_k^2(1) + c_k^2(2) + c_k^2(3) + \ldots\ldots + c_k^2(L)}{L}. \quad (11)$$

Each IMF occupies different frequency bands. Due to the chaotic behavior of ECG beats, these frequency ranges vary. By considering this point we calculated average power of each band as a feature.

All parameters are extracted from each of the selected IMFs of length 300. Therefore, feature vector length in approach one is 28 and in approach two, is 20.

2.3. Classification

In this paper, we choose sequential minimal optimization-support vector machine (SMO-SVM) for discriminating five types of heartbeats.

Support vector machine (SVM) is a popular classifier proposed by Vapnik in 1962 [56,57]. It is used for classification and regression via supervised learning. Generally, SVM is a linear classifier which fits a hyperplane such that the margin is maximized. A margin is defined as the distance between the support vectors of two different classes. The training samples from both classes near by hyperplane are called support vectors. Training SVM with more number of examples leads to a very large quadratic programming (QP) optimization problem. QP is an

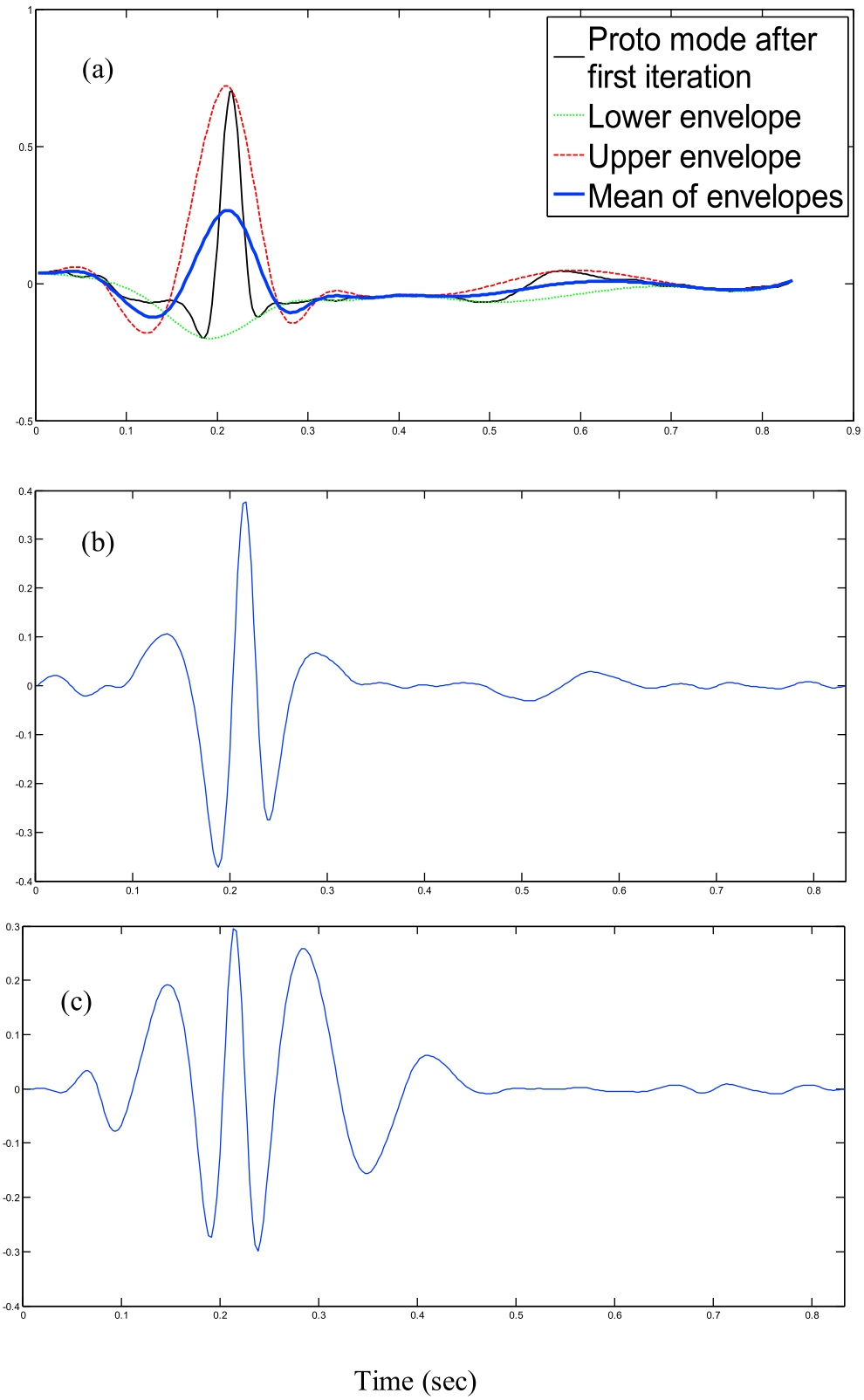

Fig. 4. Illustration of sifting process: (a) upper and lower envelopes and the mean signal of h_{11} component (b) h_{12} component (c) IMF 1 after 72 repeated siftings.

optimization technique where several variables have to be optimized subject to linear constraints [23]. Generally, numerical methods are used to solve this problem. However, it is a time-consuming process due to inner loop operations. Therefore SMO-SVM, an improved version of SVM [50] came into existence. SMO solves very large QP optimization problem analytically. It decomposes the given QP optimization problem into small QP problems. SMO-SVM selects two Lagrangian multipliers at a time and optimizes the objective function. It also adjusts the bias value based on the result. This process is repeated until selected multipliers converge. An advantage of SMO-SVM is that it can handle large training

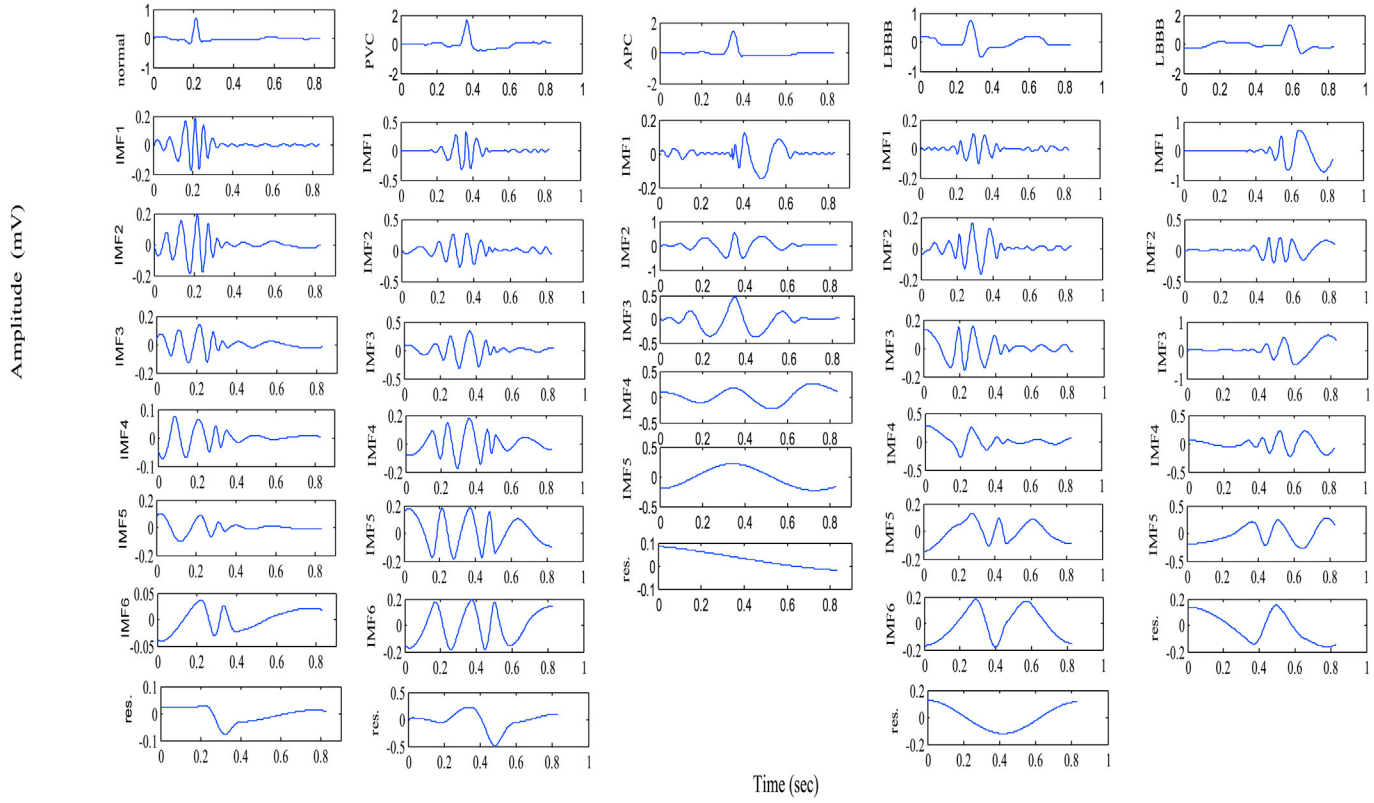

Fig. 5. Decomposition of Normal, PVC, APC, LBBB, RBBB into IMFs using EMD.

data set analytically with less computation time. SMO-SVM can also perform nonlinear classification when the patterns are inseparable in lower feature space [6]. This technique is called kernel trick in which patterns are transformed into higher dimensional space where patterns can linearly separable. In this work, we used SMO-SVM with linear, Gaussian and cubic kernels for classification.

3. Experiment

The proposed method illustrated in Fig. 1 is applied on the database specified in Section 2. We briefly explain the performance measures used to compare proposed algorithm with the other existing methods.

3.1. The performance measures

An algorithm's efficiency can be validated by choosing appropriate performance measures. Sensitivity, specificity and accuracy are the performance measures used in this work [51]. Tenfold cross-validation method is used to calculate these measures. In tenfold cross-validation, total data is divided into ten subsets. Every time one subset is used for testing and remaining 9 subsets are used for training. This folding process is repeated for ten times. Finally, average measures of all folds are computed. The advantage with tenfold cross-validation is every data example is tested exactly once. When all these measures are high, it can be assured that the classification mechanism is good.

3.2. Results

In this section, the results based on the implementation illustrated in Fig. 1 will be discussed. An important stage of the proposed method is feature extraction. Significant features are extracted from individual segmented beats of duration 830 ms. For this, we used two approaches. In the first approach, parameters described in Section 2.2.3 are extracted from IMFs using EEMD. These parameters serve as a feature vector. Statistics (median and interquartile range) of these feature vectors for each class are presented in Table 2. The variation of features, corresponding to different heartbeats can be observed from this table. Next important step is classification. The extracted feature vector is fed to the classifier to discriminate individual heartbeats. Performance measures of the classifier are evaluated using confusion matrix. Table 3 presents the confusion matrices obtained from SMO-SVM classifier with three different kernels (linear, RBF and cubic). In confusion matrix, diagonal elements represent accurately classified heartbeats. From Table 3 it is observed that SMO-SVM with cubic kernel classified more beats.

Performance measures such as specificity, sensitivity and accuracy of individual heartbeats using tenfold cross-validation are presented in Table 7. From this table, we can observe that SMO-SVM with cubic kernel classifier provides an accuracy of 99.20%, sensitivity of 98.01% and specificity of 99.49%.

Confusion matrices calculated for the second approach are shown in Table 4. Specificity, sensitivity and accuracy results calculated using SMO-SVM with three kernel functions are presented in Table 8. It is observed from Table 8, that SMO-SVM with cubic kernel provides an average accuracy of 94.68%, average sensitivity of 86.71% and average specificity of 96.67%.

These two approaches are also analyzed without denoising and the results are presented in Tables 5, 6, 9 and 10. It imperatively shows the importance of the pre-filtering for denoising.

Tables 5 and 6 show confusion matrices of approaches 1 and 2 without denoising. Performance measures in Tables 9 and 10 show that the two approaches without denoising provide results closer to the results with denoising. This proves the superiority of nonlinear feature extraction methods.

Feeding a classifier with redundant features will increase the computation cost and often degrades the performance. Therefore, selecting an optimum subset from the given set of features will enhance the abilities of a classification system. In this work, we perform correlation based feature selection to get an optimum subset of features. The

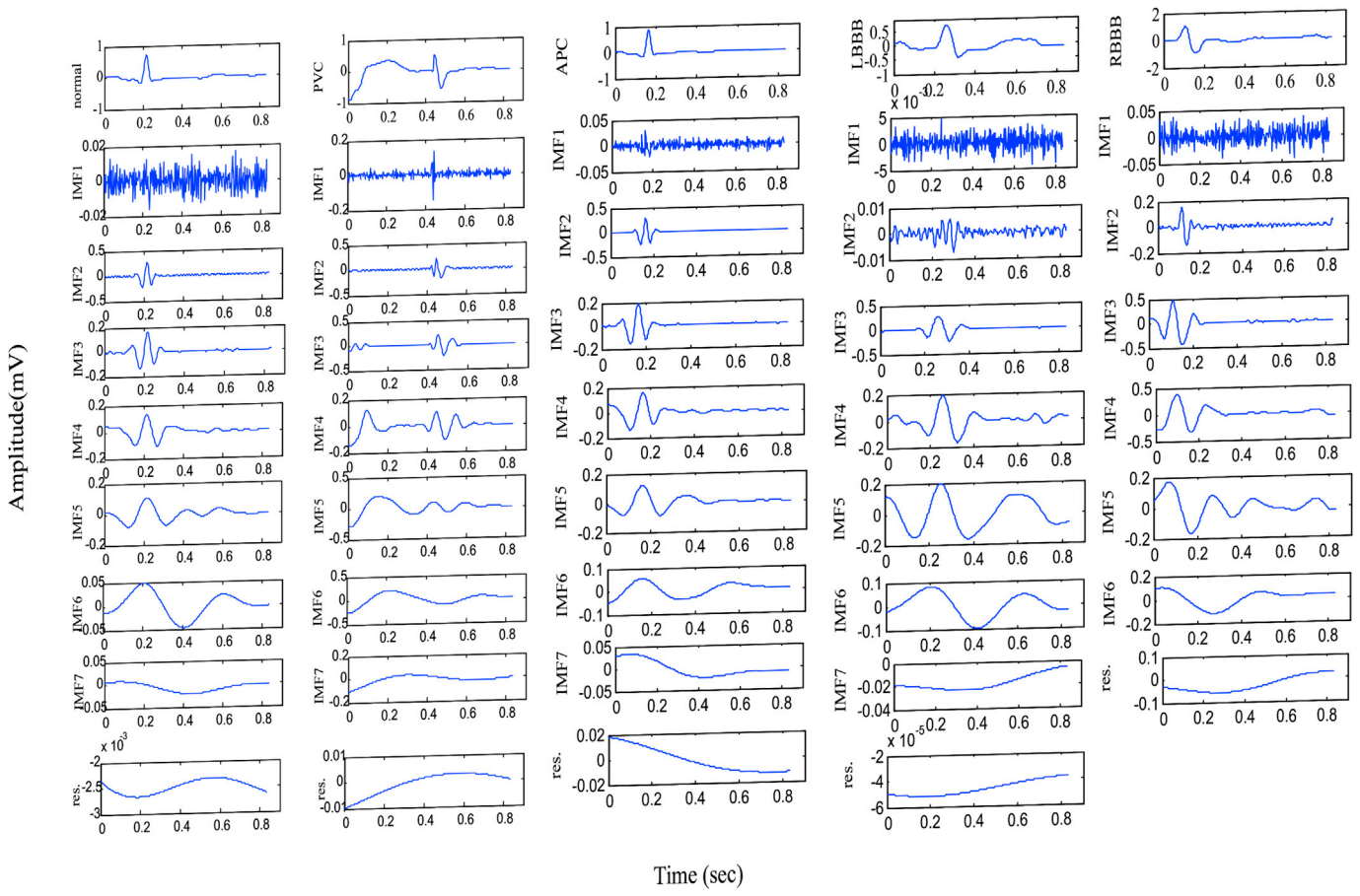

Fig. 6. Decomposition of Normal, PVC, APC, LBBB, RBBB into IMFs using EEMD.

Table 2
Median ± interquartile range of features extracted in the first approach.

Features	Normal	PVC	APC	LBBB	RBBB
SV(IMF1)	0.040694 ± 0.00923	0.35635 ± 1.135	0.02864 ± 0.0508	0.108566 ± 0.0312	0.097766 ± 0.0187
CV(IMF1)	2944.204 ± 11146.20	10869.31 ± 44250.67	3359.876 ± 15889.554	2942.871 ± 13623.40	3218.54 ± 11919.43
SEN(IMF1)	2.04953 ± 0.1818	1.1500 ± 1.629	1.9571 ± 0.3609	2.0403 ± 0.1828	2.0443 ± 0.1790
BP(IMF1)	5.21E-06 ± 2.24E-06	0.000237 ± 0.001994	5.00E-06 ± 1.48E-05	3.70E-05 ± 1.44E-05	2.95E-05 ± 1.06E-05
SV(IMF2)	0.7832 ± 0.09150	0.6699 ± 1.1694	0.3884 ± 0.3595	0.076749 ± 0.0659	0.3865 ± 0.1383
CV(IMF2)	1008.383 ± 550.466	1810.616 ± 7362.55	2242.198 ± 5751.041	2564.294 ± 9429.41	1767.721 ± 5886.35
SEN(IMF2)	0.00832 ± 0.00058	0.14874 ± 0.553	0.0505 ± 0.258	1.369 ± 0.3822	0.304 ± 0.1441
BP(IMF2)	0.0016 ± 0.00346	0.00046 ± 0.00382	0.000278 ± 0.00103	1.76E-05 ± 1.00E-05	0.000383 ± 0.000738
SV(IMF3)	0.7007 ± 0.1631	1.544 ± 0.878	0.611 ± 0.4708	2.036 ± 0.399	2.301 ± 0.419
CV(IMF3)	5942.29 ± 18637.41	1471.99 ± 5778.89	3410.442 ± 14972.11	3110.77 ± 9291.061	639.846 ± 1142.935
SEN(IMF3)	0.024 ± 0.0120	0.036 ± 0.0749	0.0944 ± 0.1841	0.026 ± 0.0139	0.030 ± 0.0257
BP(IMF3)	0.0013 ± 0.0025	0.0033 ± 0.0119	0.00092 ± 0.00259	0.01262 ± 0.0199	0.0141 ± 0.0258
SV(IMF4)	0.699 ± 0.1720	1.858 ± 1.183	0.801 ± 0.4347	1.975 ± 0.532	2.320 ± 0.4709
CV(IMF4)	1875.65 ± 9484.934	645.47 ± 3503.024	1103.03 ± 4760.688	2557.20 ± 11194.148	1193.46 ± 6307.34
SEN(IMF4)	0.091 ± 0.0430	0.0686 ± 0.0722	0.1708 ± 0.14069	0.0818 ± 0.0284	0.077 ± 0.036
BP(IMF4)	0.00132 ± 0.00217	0.0068 ± 0.01931	0.0016 ± 0.00363	0.0126 ± 0.01647	0.0147 ± 0.0224
SV(IMF5)	0.781 ± 0.1710	1.866 ± 1.1842	0.838 ± 0.5359	2.1418 ± 0.4162	1.768 ± 0.397
CV(IMF5)	838.87 ± 3324.393	272.90 ± 999.475	279.282 ± 1273.1428	219.38 ± 719.7034	574.9640999 ± 2829.609
SEN(IMF5)	0.1615 ± 0.05496	0.102 ± 0.0746	0.185 ± 0.1084	0.1642 ± 0.0379	0.190 ± 0.0577
BP(IMF5)	0.0019 ± 0.00261	0.00878 ± 0.02025	0.00185 ± 0.00341	0.0145 ± 0.01474	0.00875 ± 0.0123
SV(IMF6)	0.5806 ± 0.1826	1.968 ± 1.7088	0.654 ± 0.45191	2.459 ± 0.4232	1.058 ± 0.3279
CV(IMF6)	158.88 ± 720.24	81.41 ± 288.13	111.90 ± 488.622	207.98 ± 815.911	138.790 ± 532.55
SEN(IMF6)	0.151 ± 0.0407	0.0925 ± 0.0569	0.1208 ± 0.0682	0.1432 ± 0.0226	0.114 ± 0.0358
BP(IMF6)	0.0010 ± 0.00103	0.0118 ± 0.0294	0.0013 ± 0.002447	0.022 ± 0.0140	0.0034 ± 0.00382
SV(IMF7)	0.481 ± 0.1421	1.8621 ± 1.3780	0.3708 ± 0.293	1.353 ± 0.4369	0.992 ± 0.3196
CV(IMF7)	72.400 ± 269.157	38.66 ± 185.129	29.17 ± 128.188	45.12 ± 176.003	122.68 ± 525.935
SEN(IMF7)	0.0800 ± 0.0410	0.0518 ± 0.0410	0.0519 ± 0.0425	0.0503 ± 0.0192	0.0390 ± 0.0146
BP(IMF7)	0.00075 ± 0.000817	0.00772 ± 0.0201	0.00032 ± 0.000706	0.0048 ± 0.00367	0.00276 ± 0.00187

Note: SV-singular value, CV-coefficient of variation, SEN- sample entropy, BP-band power.

feature selection scheme evaluates the merit of a feature by measuring Pearson's correlation coefficient between selected feature and class. Later it assigns ranks to each feature using ranker search method. The importance of feature selection is demonstrated on approach one (with and

Table 3
Confusion matrices with different kernels for SMO-SVM: first approach.

	SMO-SVM Linear					SMO-SVM RBF					SMO-SVM Cubic				
	Normal	PVC	APC	LBBB	RBBB	Normal	PVC	APC	LBBB	RBBB	Normal	PVC	APC	LBBB	RBBB
Normal	1959	1	38	0	2	1959	10	31	0	0	1980	1	18	0	1
PVC	5	1753	202	26	14	1	1908	83	4	4	0	1959	35	2	4
APC	99	122	1675	14	90	24	85	1838	1	52	1	68	1905	3	23
LBBB	2	37	6	1949	6	0	27	3	1969	1	0	17	3	1978	2
RBBB	1	14	13	5	1967	0	12	14	2	1972	1	7	9	4	1979

Table 4
Confusion matrices with different kernels for SMO-SVM: second approach.

	SMO-SVM Linear					SMO-SVM RBF					SMO-SVM Cubic				
	Normal	PVC	APC	LBBB	RBBB	Normal	PVC	APC	LBBB	RBBB	Normal	PVC	APC	LBBB	RBBB
Normal	1838	10	140	2	10	1837	18	126	1	18	1841	10	134	2	13
PVC	106	779	332	396	387	35	1537	195	104	129	30	1426	235	144	165
APC	419	56	1232	157	136	155	131	1546	47	121	20	87	1708	52	133
LBBB	0	205	26	1744	25	0	101	18	1867	14	0	62	36	1886	16
RBBB	26	213	35	103	1623	9	125	47	22	1797	12	93	60	25	1810

without denoising). Overall accuracy values for all feature subsets with cubic kernel are presented in Figs. 7 and 8. Subsets are determined based on ranking. It is observed from the results that there is no significant performance improvement in classification after 12- dimensional feature subset for the first approach with denoising and 16 dimensional feature subset for the approach one without denoising. Performance measures of approach one (with and without denoising) on selected features are presented in Tables 11 and 12.

In addition, to substantiate the performance of our proposed method (approach one) we tested it on another database: INCART [18]. We consider four types of heartbeats for our analysis: normal (1000), PVC (1000), APC (1000) and RBBB (1000).

Confusion matrices calculated for the first approach on INCART are shown in Table 13. Performance measures calculated using SMO-SVM with three kernel functions are presented in Table 14. From the results, we can observe that SMO-SVM with cubic kernel yields 95.5% of sensitivity, 98.37% of specificity and accuracy of 97.57%.

3.3. Discussion

Proposed method is primarily studied on MIT-BIH arrhythmia database. Later, to assess the effectiveness of the first approach, we applied it on INCART. According to AAMI standards and recommendations, all the heartbeats in the MIT data set are grouped into five classes. Heartbeats are classified as ectopic or non-ectopic beats. However, this is not always desirable. Particular types of arrhythmias can be diagnosed by identifying the corresponding irregular heartbeats. Some scenarios are presented below.

1. Ventricular bigeminy, trigeminy and tachycardia are identified based on the frequency of PVC beats.
2. Repeated APC beats will turn into dangerous arrhythmias such as atrial flutter and atrial fibrillation when a patient has underlying structural heart problems. According to AAMI standards and recommendations, PVCs are grouped in with ventricular flutter and escape beats. Similarly, APCs are grouped in with other premature beats, such as aberrated atrial, supraventricular, and nodal beats. Therefore, discrimination of the required beats is not possible.
3. Sometimes, there is a stoppage or a pause along the electrical impulse pathway from the atrium to the ventricles due to BBB. This results in a poor blood-pumping mechanism. Often, these BBBs also show underlying heart problems. According to AAMI standards and recommendations, BBBs are grouped together with normal beats under the classification of non-ectopic beats. Therefore, it is not possible to differentiate normal heartbeats from BBBs.

In this study, we considered five types of heartbeats (2000 normal, 2000 PVC, 2000 APC, 2000 LBBB, and 2000 RBBB). The MIT dataset is dominated by normal beats, but we chose a part with normal beats to avoid bias in the classification. Remaining beats were chosen appropriately to avoid bias toward any one of the classes. Similarly, we considered four types of heartbeats (1000 normal, 1000 PVC, 1000 APC, and 1000 RBBB) from INCART. The proposed method effectively classified ectopic and bundle branch block beats and provides substantial results in terms of specificity, sensitivity and accuracy. EMD, EEMD decomposes a signal based on its nature. Hence any type of ECG signal can be efficiently represented. Loss of information is minimum in this case. Features were able to extract the nature of the signal effectively. The chaotic behavior of the ECG signal is well analyzed by the representation scheme.

To assess the performance of proposed methodology, we compared it with the existing methods in the literature. Ham and Han [20] classified normal and PVC beats using fuzzy ARTMAP architecture where the linear prediction coefficients (LPC) and mean square of the QRS segments are the selected features. Specificity of 99% and sensitivity of 97% was achieved in this approach. Yeh et al. [63] employed the linear discriminant analysis along with qualitative features to classify five types of heartbeats namely normal, PVC, APC, LBBB, and RBBB and achieved an accuracy of 98.97%, 92.63%, 84.68%, 91.07%, 95.09% respectively and

Table 5
Confusion matrices with different kernels for SMO-SVM: first approach without denoising.

	SMO-SVM Linear					SMO-SVM RBF					SMO-SVM Cubic				
	Normal	PVC	APC	LBBB	RBBB	Normal	PVC	APC	LBBB	RBBB	Normal	PVC	APC	LBBB	RBBB
Normal	1951	2	47	0	0	1951	12	37	0	0	1967	4	29	0	0
PVC	5	1764	176	30	25	0	1899	84	6	11	3	1948	38	3	8
APC	119	147	1637	8	89	30	106	1795	2	67	49	91	1786	4	70
LBBB	0	55	4	1940	1	0	42	2	1955	1	0	28	2	1968	2
RBBB	0	14	9	1	1976	0	24	11	0	1965	0	7	17	1	1975

Table 6
Confusion matrices with different kernels for SMO-SVM: second approach without denoising.

	SMO-SVM Linear					SMO-SVM RBF					SMO-SVM Cubic				
	Normal	PVC	APC	LBBB	RBBB	Normal	PVC	APC	LBBB	RBBB	Normal	PVC	APC	LBBB	RBBB
Normal	1897	6	91	6	0	1889	29	75	6	11	1920	9	64	5	2
PVC	53	1052	328	208	359	29	1433	237	111	190	30	1369	286	115	200
APC	175	131	1484	80	130	95	194	1549	54	108	98	168	1553	50	131
LBBB	20	91	51	1807	31	12	123	34	1804	27	11	76	31	1860	22
RBBB	0	113	101	4	1782	0	124	52	3	1821	3	94	66	9	1828

Table 7
Performance measures of SMO-SVM with various kernels: first approach.

	SMO-SVM Linear			SMO-SVM RBF			SMO-SVM Cubic		
	Sensitivity %	Specificity %	Accuaracy %	Sensitivity %	Specificity %	Accuaracy %	Sensitivity %	Specificity %	Accuaracy %
Normal	98	98.66	98.52	98.00	99.17	99.34	99.00	99.97	99.78
PVC	87.6	97.82	95.79	95.4	98.32	97.74	97.95	98.83	98.66
APC	83.80	96.79	95.01	91.9	98.36	97.07	95.25	99.18	98.40
LBBB	97.50	99.36	99.04	98.5	99.91	99.62	98.90	99.88	99.69
RBBB	98.40	99.58	98.55	98.6	99.28	99.15	98.95	99.63	99.50
Average	93.06	98.44	97.44	96.48	99.00	98.58	98.01	99.49	99.20

Table 8
Performance measures of SMO-SVM with various kernels: second approach.

	SMO-SVM Linear			SMO-SVM RBF			SMO-SVM Cubic		
	Sensitivity %	Specificity %	Accuaracy %	Sensitivity %	Specificity %	Accuaracy %	Sensitivity %	Specificity %	Accuaracy %
Normal	91.9	93.43	93.13	91.8	97.51	96.38	92.05	99.22	97.79
PVC	39.00	93.95	82.95	76.8	95.31	91.62	71.3	96.85	91.74
APC	61.6	93.33	86.99	77.3	95.17	91.60	85.40	94.18	92.45
LBBB	87.20	91.77	90.86	93.30	97.82	96.93	94.30	97.21	96.63
RBBB	81.2	93.02	88.91	89.8	96.47	95.15	90.5	95.91	94.83
Average	72.18	93.10	89.86	85.80	98.81	96.45	86.71	96.67	94.68

Table 9
Performance measures of SMO-SVM with various kernels: first approach without denoising.

	SMO-SVM Linear			SMO-SVM RBF			SMO-SVM Cubic		
	Sensitivity %	Specificity %	Accuaracy %	Sensitivity %	Specificity %	Accuaracy %	Sensitivity %	Specificity %	Accuaracy %
Normal	97.5	98.45	98.27	97.50	99.62	99.21	98.35	99.35	99.15
PVC	88.72	97.27	95.46	95.00	97.7	97.15	97.40	98.37	98.18
APC	81.8	97.05	94.01	89.80	98.32	96.61	89.30	98.92	97.00
LBBB	97.00	99.51	99.01	97.80	99.90	99.47	98.40	99.99	99.60
RBBB	98.8	98.56	98.61	98.31	99.01	98.86	98.95	99.00	98.95
Average	92.76	98.16	97.07	95.36	98.91	98.53	96.48	99.12	98.57

Table 10
Performance measures of SMO-SVM with various kernels: second approach without denoising.

	SMO-SVM Linear			SMO-SVM RBF			SMO-SVM Quadratic		
	Sensitivity %	Specificity %	Accuaracy %	Sensitivity %	Specificity %	Accuaracy %	Sensitivity %	Specificity %	Accuaracy %
Normal	94.8	96.9	96.49	94.50	98.30	97.53	96.00	98.22	97.78
PVC	52.6	86.85	80	71.70	94.12	89.63	68.5	95.66	90.22
APC	74.20	81.45	80	77.5	95.02	91.51	77.60	94.41	91.06
LBBB	90.32	96.27	95.09	90.2	97.82	96.30	93.76	97.76	96.81
RBBB	89.10	93.50	92.62	91.00	95.92	94.95	91.40	95.56	94.73
Average	80.20	90.99	88.84	84.98	96.23	93.97	85.45	96.32	94.12

a total accuracy of 96.23%. Khazaee and Ebrahimzadeh [30] classified normal, PVC, APC, LBBB and RBBB beats using the genetic algorithm-support vector machine together with spectral and temporal features and achieved 96% accuracy. Yu and Chen [64] performed heartbeat classification of noisy ECG signals with the help of higher order statistical features computed from wavelet transform subbands and three RR interval feature set using the neural network and obtained overall accuracy of 97.5%. Yeh et al. [62] used the cluster analysis for classifying five types of ECG beats namely normal, APC, PVC, RBBB, LBBB and attained 95.59%, 93.77%, 94.51%, 90.50% and 91.32% sensitivity and overall classification accuracy of about 94.30%. Martis et al. [40] used principal components of the segmented ECG beat as a feature to the least

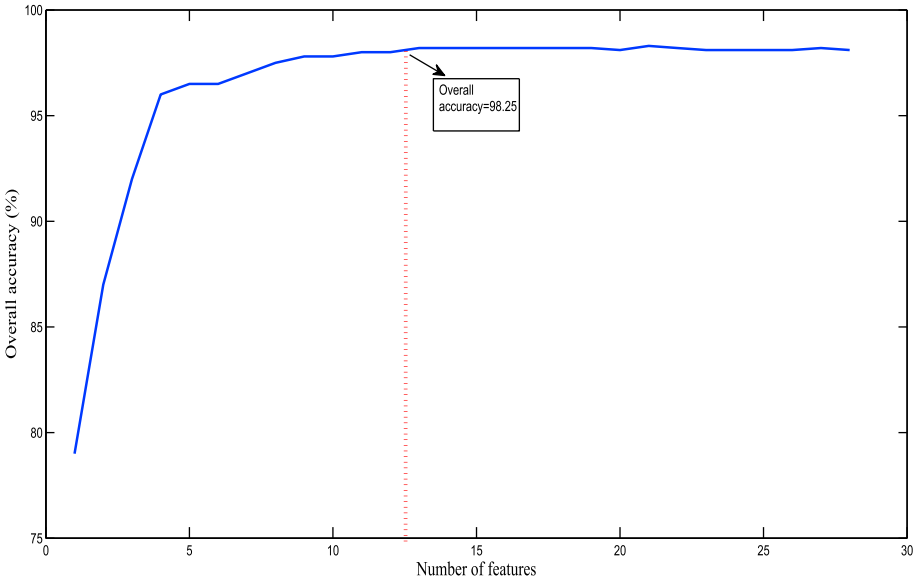

Fig. 7. Overall accuracies for different number of features selected using correlation based feature selection: first approach with denoising.

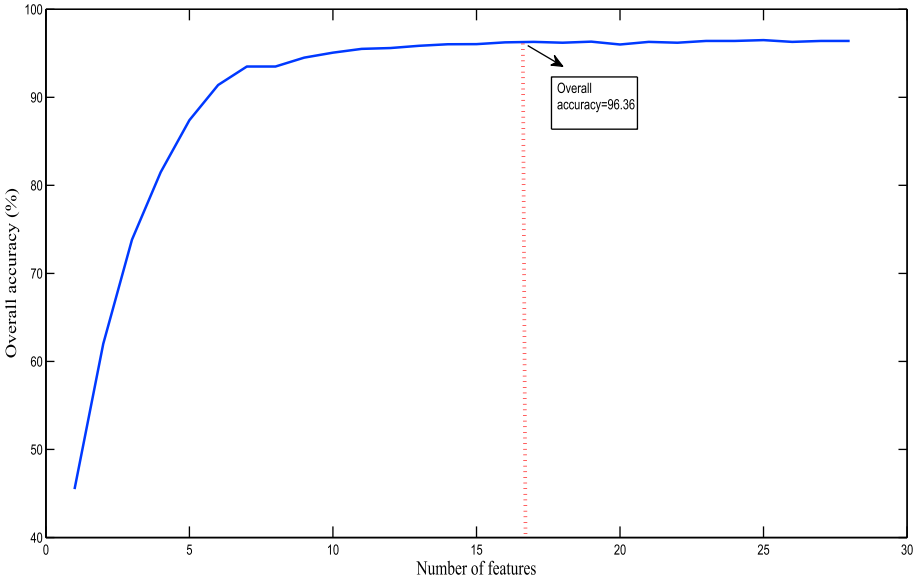

Fig. 8. Overall accuracies for different number of features selected using correlation based feature selection: first approach without denoising.

Table 11
Average performance measures of ten-folds SMO-SVM: first approach with denoising (selected 12 features).

	SMO-SVM Cubic		
	Sensitivity %	Specificity %	Accuracy %
Normal	99.35	99.7	99.63
PVC	97.55	99.27	98.93
APC	95.50	99.35	98.58
LBBB	99.10	99.91	99.75
RBBB	99.00	99.38	99.31
Average	98.10	99.52	99.24

squares-support vector machine (LS-SVM) classifier to classify five kinds of heartbeats and procured 99.90%, 99.10% and 98.11% of average sensitivity, specificity and accuracy respectively. Thomas et al. [55] employed a novel feature set containing complex wavelet coefficients extracted from dual-tree complex wavelet transform (DTCWT) integrated with four other features, namely AC power, kurtosis, skewness and timing information to classify five types of ECG beats using feed forward neural network and obtained an overall sensitivity of 97.80%. Martis et al. [41] used bispectrum and classified five classes of ECG beats using LS-SVM and reported 98.31%, 99.27% and 93.48% of average specificity, sensitivity and accuracy of respectively. Khalaf et al. [29] estimated the spectral correlation coefficients through cyclostationary signal analysis

Table 12
Average performance measures of ten-folds SMO-SVM: first approach without denoising (selected 16 features).

	SMO-SVM Cubic		
	Sensitivity %	Specificity %	Accuracy %
Normal	98.5	99.27	99.12
PVC	97.25	98.28	99.08
APC	88.95	98.97	96.97
LBBB	98.00	99.87	99.50
RBBB	99.1	98.91	98.95
Average	96.36	99.06	98.72

Table 13
Confusion matrices with different kernels for SMO-SVM: first approach with INCART.

	SMO-SVM Linear				SMO-SVM RBF				SMO-SVM Cubic			
	Normal	PVC	APC	RBBB	Normal	PVC	APC	RBBB	Normal	PVC	APC	RBBB
Normal	986	7	6	1	979	19	2	0	992	5	3	0
PVC	7	907	75	11	1	937	52	10	8	926	55	11
APC	5	33	869	93	1	43	910	46	1	39	916	44
RBBB	0	1	33	966	0	11	18	971	1	3	24	972

Table 14
Performance measures of SMO-SVM with various kernels: first approach with INCART.

	SMO-SVM Linear			SMO-SVM RBF			SMO-SVM Cubic		
	Sensitivity %	Specificity %	Accuaracy %	Sensitivity %	Specificity %	Accuaracy %	Sensitivity %	Specificity %	Accuaracy %
Normal	98.60	99.60	99.35	97.90	99.93	99.42	99.20	99.66	99.55
PVC	90.70	98.63	96.65	93.70	97.56	96.60	92.60	98.43	96.97
APC	86.90	96.20	93.87	91.0	97.60	95.95	91.60	97.26	95.85
RBBB	96.60	96.50	96.52	97.10.8	98.13	97.87	97.20	98.16	97.92
Average	93.20	97.73	96.59	94.92	98.30	97.46	95.15	98.37	97.57

approach and employed SVM to classify five types of heartbeats such as (normal, PVC, APC, RBBB, LBBB) and 99.20% of sensitivity, 99.70% of specificity and 98.60% of accuracy are obtained.

From Table 7 it is evident that the proposed methodology achieved appreciable performance measures of 98.01% average sensitivity, 99.49% average specificity and average accuracy of 99.20%. Also, results obtained from INCART database supported the fairness and significance of the proposed method for heartbeat classification. The performance of our method is significant even without denoising. This justifies the superiority of the nonlinear features in ECG heartbeat classification.

3.4. Limitations and future scope

The study was conducted on five types of beats only. To generalize the results various types and numerous beats should be incorporated. There is a possibility of intra-patient paradigm, i.e. chance of same patient details presented in both training and testing data. This may lead to biased result to some extent. Utilization of a fixed beat length is not always desirable due to fast and slow varying heart rhythms. There is a need to study adaptive beat size segmentation. Another important limitation is in understanding the exact relation between underlying physiology and features. There is no clue about which features diagnose a disease. Therefore, feature based disease identification is a significant research area for future study.

4. Conclusion

Automated classification of ECG heartbeats is the objective of this work. In this paper, we have proposed nonlinear decomposition based feature extraction methods for classifying five types of heartbeats namely, normal, APC, PVC, LBBB, RBBB. Two approaches were developed and their performance was evaluated using MIT-BIH and INCART databases. In the first approach, EEMD based features were extracted from ECG signals. In the second approach, EMD based features were extracted. These features were fed to an SMO-SVM for classification. The first approach achieved better classification results. This approach showed its ability to discriminate different types of heartbeats even under noisy conditions.

Conflicts of interest statement

The authors have NO affiliations with or involvement in any organization or entity with any financial interest (such as honoraria; educational grants; participation in speakers' bureaus; membership, employment, consultancies, stock ownership, or other equity interest; and expert testimony or patent-licensing arrangements), or non-financial interest (such as personal or professional relationships, affiliations, knowledge or beliefs) in the subject matter or materials discussed in this manuscript.

Acknowledgement

We thank the editor-in-chief and the reviewers for their valuable inputs. We are grateful to Dr. G. R. Reddy, Dr. S. Sridevi of VIT University, for improving the presentation of the manuscript. We sincerely acknowledge the American manuscript editors who helped in refining the language of the manuscript.

References

[1] V.X. Afonso, W.J. Tompkins, Detecting ventricular fibrillation, IEEE Eng. Med. Biol. Mag. 14 (2) (1995) 152–159.
[2] V.X. Afonso, W.J. Tompkins, T.Q. Nguyen, S. Luo, Ecg beat detection using filter banks, IEEE Trans. Biomed. Eng. 46 (2) (1999) 192–202.

[3] A. Al-Fahoum, I. Howitt, Combined wavelet transformation and radial basis neural networks for classifying life-threatening cardiac arrhythmias, Med. Biol. Eng. Comput. 37 (5) (1999) 566–573.
[4] F. Alonso-Atienza, E. Morgado, L. Fernandez-Martinez, A. Garcia-Alberola, J.L. Rojo-Alvarez, Detection of life-threatening arrhythmias using feature selection and support vector machines, IEEE Trans. Biomed. Eng. 61 (3) (2014) 832–840.
[5] A. Amann, R. Tratnig, K. Unterkofler, et al., Reliability of old and new ventricular fibrillation detection algorithms for automated external defibrillators, Biomed. Eng. Online 4 (1) (2005) 60.
[6] B.E. Boser, I.M. Guyon, V.N. Vapnik, A training algorithm for optimal margin classifiers, in: Proceedings of the Fifth Annual Workshop on Computational Learning Theory, ACM, 1992, pp. 144–152.
[7] G. Braccini, L. Edenbrandt, M. Lagerholm, C. Peterson, O. Rauer, R. Rittner, L. Sörnmo, Self-organizing maps and hermite functions for classification of ecg complexes, in: Computers in Cardiology 1997, IEEE, 1997, pp. 425–428.
[8] C.E. Brown, Coefficient of variation, in: Applied Multivariate Statistics in Geohydrology and Related Sciences, Springer, 1998, pp. 155–157.
[9] C.-D. Chang, C.-C. Wang, B.C. Jiang, Singular value decomposition based feature extraction technique for physiological signal analysis, J. Med. Syst. 36 (3) (2012) 1769–1777.
[10] K.-M. Chang, S.-H. Liu, Gaussian noise filtering from ecg by wiener filter and ensemble empirical mode decomposition, J. Signal Process. Syst. 64 (2) (2011) 249–264.
[11] F. Chiarugi, D. Emmanouilidou, I. Tsamardinos, I. Tollis, Morphological classification of heartbeats using similarity features and a two-phase decision tree, in: Computers in Cardiology, 2008, IEEE, 2008, pp. 849–852.
[12] M.A. Colominas, G. Schlotthauer, M.E. Torres, Improved complete ensemble emd: a suitable tool for biomedical signal processing, Biomed. Signal Process. Control 14 (2014) 19–29.
[13] P. De Chazal, M.O. Dwyer, R.B. Reilly, Automatic classification of heartbeats using ecg morphology and heartbeat interval features, IEEE Trans. Biomed. Eng. 51 (7) (2004) 1196–1206.
[14] N. Emanet, Ecg beat classification by using discrete wavelet transform and random forest algorithm, in: Soft Computing, Computing with Words and Perceptions in System Analysis, Decision and Control, 2009. ICSCCW 2009. Fifth International Conference on, IEEE, 2009, pp. 1–4.
[15] Z. Feng, M. Liang, Y. Zhang, S. Hou, Fault diagnosis for wind turbine planetary gearboxes via demodulation analysis based on ensemble empirical mode decomposition and energy separation, Renew. Energy 47 (2012) 112–126.
[16] P. Flandrin, Emd Matlab 7.1 Codes with Examples, 2007.
[17] J. Gilles, Empirical wavelet transform, IEEE Trans. Signal Process. 61 (16) (2013) 3999–4010.
[18] A.L. Goldberger, et al., Components of a new research resource for complex physiologic signals, physiobank, physiotoolkit, and physionet, american heart association journals, Circulation 101 (23) (2000) 1–9.
[19] G.H. Golub, C. Reinsch, Singular value decomposition and least squares solutions, Numer. Math. 14 (5) (1970) 403–420.
[20] F.M. Ham, S. Han, Classification of cardiac arrhythmias using fuzzy artmap, IEEE Trans. Biomed. Eng. 43 (4) (1996) 425–429.
[21] H.G. Hosseini, K. Reynolds, D. Powers, A multi-stage neural network classifier for ecg events, in: Engineering in Medicine and Biology Society, 2001. Proceedings of the 23rd Annual International Conference of the IEEE, vol. 2, IEEE, 2001, pp. 1672–1675.
[22] N.E. Huang, Z. Shen, S.R. Long, M.C. Wu, H.H. Shih, Q. Zheng, N.-C. Yen, C.C. Tung, H.H. Liu, The empirical mode decomposition and the hilbert spectrum for nonlinear and non-stationary time series analysis, in: Proceedings of the Royal Society of London a: Mathematical, Physical and Engineering Sciences, vol. 454, The Royal Society, 1998, pp. 903–995.
[23] F.R. Jacobs, R.B. Chase, Operations and Supply Chain Management: the Core, McGraw-Hill, 2013.
[24] S. Kadambe, R. Murray, G.F. Boudreaux-Bartels, Wavelet transform-based qrs complex detector, IEEE Trans. Biomed. Eng. 46 (7) (1999) 838–848.
[25] A. Karagiannis, P. Constantinou, Noise-assisted data processing with empirical mode decomposition in biomedical signals, IEEE Trans. Inf. Technol. Biomed. 15 (1) (2011) 11–18.
[26] S. Karimifard, A. Ahmadian, M. Khoshnevisan, M. Nambakhsh, Morphological heart arrhythmia detection using hermitian basis functions and knn classifier, in: Engineering in Medicine and Biology Society, 2006. EMBS'06. 28th Annual International Conference of the IEEEIEEE, 2006, pp. 1367–1370.
[27] L. Khadra, A. Al-Fahoum, H. Al-Nashash, Detection of life-threatening cardiac arrhythmias using the wavelet transformation, Med. Biol. Eng. Comput. 35 (6) (1997) 626–632.
[28] L. Khadra, A.S. Al-Fahoum, S. Binajjaj, A quantitative analysis approach for cardiac arrhythmia classification using higher order spectral techniques, IEEE Trans. Biomed. Eng. 52 (11) (2005) 1840–1845.
[29] A.F. Khalaf, M.I. Owis, I.A. Yassine, A novel technique for cardiac arrhythmia classification using spectral correlation and support vector machines, Expert Syst. Appl. 42 (21) (2015) 8361–8368.
[30] A. Khazaee, A. Ebrahimzadeh, Classification of electrocardiogram signals with support vector machines and genetic algorithms using power spectral features, Biomed. Signal Process. Control 5 (4) (2010) 252–263.
[31] Y. Kutlu, D. Kuntalp, Feature extraction for ecg heartbeats using higher order statistics of wpd coefficients, Comput. Methods Programs Biomed. 105 (3) (2012) 257–267.
[32] Y. Lei, Z. He, Y. Zi, Application of the eemd method to rotor fault diagnosis of rotating machinery, Mech. Syst. Signal Process. 23 (4) (2009) 1327–1338.
[33] Y. Lei, Z. He, Y. Zi, Eemd method and wnn for fault diagnosis of locomotive roller bearings, Expert Syst. Appl. 38 (6) (2011) 7334–7341.
[34] H. Li, X. Feng, L. Cao, E. Li, H. Liang, X. Chen, A new ecg signal classification based on wpd and apen feature extraction, Circuits Syst. Signal Process. 35 (1) (2016) 339–352.
[35] H. Li, W. Han, C. Hu, M.Q. Meng, Detecting ventricular fibrillation by fast algorithm of dynamic sample entropy, in: Robotics and Biomimetics (ROBIO), 2009 IEEE International Conference on, IEEE, 2009, pp. 1105–1110.
[36] K.P. Lin, W.H. Chang, Qrs feature extraction using linear prediction, IEEE Trans. Biomed. Eng. 36 (10) (1989) 1050–1055.
[37] P. Lovie, Coefficient of variation, in: Encyclopedia of Statistics in Behavioral Science, 2005.
[38] J.P. Martínez, R. Almeida, S. Olmos, A.P. Rocha, P. Laguna, A wavelet-based ecg delineator: evaluation on standard databases, IEEE Trans. Biomed. Eng. 51 (4) (2004) 570–581.
[39] R.J. Martis, U.R. Acharya, H. Adeli, Current methods in electrocardiogram characterization, Comput. Biol. Med. 48 (2014) 133–149.
[40] R.J. Martis, U.R. Acharya, K. Mandana, A.K. Ray, C. Chakraborty, Application of principal component analysis to ecg signals for automated diagnosis of cardiac health, Expert Syst. Appl. 39 (14) (2012) 11792–11800.
[41] R.J. Martis, U.R. Acharya, K. Mandana, A.K. Ray, C. Chakraborty, Cardiac decision making using higher order spectra, Biomed. Signal Process. Control 8 (2) (2013) 193–203.
[42] R.J. Martis, U.R. Acharya, A.K. Ray, C. Chakraborty, Application of higher order cumulants to ecg signals for the cardiac health diagnosis, in: Engineering in Medicine and Biology Society, EMBC, 2011 Annual International Conference of the IEEE, IEEE, 2011, pp. 1697–1700.
[43] S. Mendis, P. Puska, B. Norrving, et al., Global Atlas on Cardiovascular Disease Prevention and Control, World Health Organization, 2011.
[44] K.-i. Minami, H. Nakajima, T. Toyoshima, Real-time discrimination of ventricular tachyarrhythmia with fourier-transform neural network, IEEE Trans. Biomed. Eng. 46 (2) (1999) 179–185.
[45] G.B. Moody, R.G. Mark, The impact of the mit-bih arrhythmia database, IEEE Eng. Med. Biol. Mag. 20 (3) (2001) 45–50.
[46] I.S. Murthy, M.R. Rangaraj, New concepts for pvc detection, IEEE Trans. Biomed. Eng. 7 (1979) 409–416.
[47] J. Nadal, M. de C Bossan, Classification of cardiac arrhythmias based on principal component analysis and feedforward neural networks, in: Computers in Cardiology 1993, Proceedings, IEEE, 1993, pp. 341–344.
[48] S. Osowski, T.H. Linh, Ecg beat recognition using fuzzy hybrid neural network, IEEE Trans. Biomed. Eng. 48 (11) (2001) 1265–1271.
[49] J. Pan, W.J. Tompkins, A real-time qrs detection algorithm, IEEE Trans. Biomed. Eng. 3 (1985) 230–236.
[50] J.C. Platt, 12 fast training of support vector machines using sequential minimal optimization, Adv. Kernel Methods (1999) 185–208.
[51] D.M. Powers, Evaluation: from Precision, Recall and f-measure to Roc, Informedness, Markedness and Correlation, 2011.
[52] R.M. Rangayyan, Biomedical Signal Analysis, vol. 33, John Wiley & Sons, 2015.
[53] J.S. Richman, J.R. Moorman, Physiological time-series analysis using approximate entropy and sample entropy, Am. J. Physiol. Heart Circ. Physiol. 278 (6) (2000) H2039–H2049.
[54] I. Saini, D. Singh, A. Khosla, Electrocardiogram beat classification using empirical mode decomposition and multiclass directed acyclic graph support vector machine, Comput. Electr. Eng. 40 (5) (2014) 1774–1787.
[55] M. Thomas, M.K. Das, S. Ari, Classification of cardiac arrhythmias based on dual tree complex wavelet transform, in: Communications and Signal Processing (ICCSP), 2014 International Conference on, IEEE, 2014, pp. 729–733.
[56] A.C.G. Thome, Svm Classifiers-Concepts and Applications to Character Recognition, INTECH Open Access Publisher, 2012.
[57] V.N. Vapnik, V. Vapnik, Statistical Learning Theory, vol. 1, Wiley New York, 1998.
[58] T. Wang, M. Zhang, Q. Yu, H. Zhang, Comparing the applications of emd and eemd on time–frequency analysis of seismic signal, J. Appl. Geophys. 83 (2012) 29–34.
[59] Z. Wu, N.E. Huang, Ensemble empirical mode decomposition: a noise-assisted data analysis method, Adv. Adapt. Data Anal. 1 (01) (2009) 1–41.
[60] M. Yang, Y. Tian, H. Wang, Review of the Ecg Signal Identification System Design, 2015.
[61] C. Ye, B.V. Kumar, M.T. Coimbra, Heartbeat classification using morphological and dynamic features of ecg signals, IEEE Trans. Biomed. Eng. 59 (10) (2012) 2930–2941.
[62] Y.-C. Yeh, C.W. Chiou, H.-J. Lin, Analyzing ecg for cardiac arrhythmia using cluster analysis, Expert Syst. Appl. 39 (1) (2012) 1000–1010.
[63] Y.-C. Yeh, W.-J. Wang, C.W. Chiou, Cardiac arrhythmia diagnosis method using linear discriminant analysis on ecg signals, Measurement 42 (5) (2009) 778–789.
[64] S.-N. Yu, Y.-H. Chen, Noise-tolerant electrocardiogram beat classification based on higher order statistics of subband components, Artif. Intell. Med. 46 (2) (2009) 165–178.